Chemical Physics Letters 655–656 (2016) 11–16

Contents lists available at ScienceDirect

Chemical Physics Letters

journal homepage: www.elsevier.com/locate/cplett

Research paper

Formation of stable cell–cell contact without a solid/gel scaffold: Non-invasive manipulation by laser under depletion interaction with a polymer

Shu Hashimoto, Aoi Yoshida, Taeko Ohta, Hiroaki Taniguchi, Koichiro Sadakane *, Kenichi Yoshikawa *

Faculty of Life and Medical Sciences, Doshisha University, Kyotanabe 610-0394, Japan

ARTICLE INFO

Article history:
Received 5 February 2016
Revised 9 May 2016
In final form 9 May 2016
Available online 10 May 2016

Keywords:
Optical tweezers
Depletion effect
Cell–cell adhesion
Crowding effect

ABSTRACT

We report a novel method for constructing a stable three-dimensional cellular assembly in the absence of a solid or gel scaffold. A targeted cell was transferred to another cell, and the two were kept in contact for a few minutes by optical manipulation in an aqueous medium containing a hydrophilic polymer. Interestingly, this cell–cell adhesion was maintained even after elimination of the polymer. We discuss the mechanism of the formation of stable multi-cellular adhesion in terms of spontaneous rearrangement of the components embedded in the pair of facing membranes.

1. Introduction

The fabrication of three-dimensional (3-D) cellular assembly systems with multiple cells through the desired positioning of individual cells has become increasingly important with recent developments regarding the outcome of cell differentiation as well as the discovery of dedifferentiation techniques using induced pluripotent stem cells (iPSCs) and embryonic stem cells (ESCs) [1–4]. To achieve this end, a chemically controlled gel has frequently been applied as a scaffold to achieve a 3-D cellular assembly [5–8]. Additionally, various other approaches such as magnetic liposomes [9], polymeric aqueous two-phase systems [10], printing of cells with polymers [11] and well-controlled micro-arrays of a solid substrate [12] have been proposed. Unfortunately, artificial scaffolds and/or artificial chemical substances are thus far indispensable for the assembly of cells, and such xenobiotics may have non-negligible effects on the structure and function of the assembled cells. As a noninvasive method of cell manipulation in bulk aqueous medium under remote control, laser tweezers [13] have been applied for the transport of targeted cells in aqueous medium [14,15]. Although the use of laser tweezers is a well-known method for transferring a targeted cell, it has been difficult to sustain stable cell–cell contact after the laser is switched off. Living mammalian cells are usually suspended in an aqueous solution and tend to dissociate due to repulsive interactions between the facing membrane surfaces [16]. Under these circumstances, the current methodologies for cellular assembly are mostly restricted to the adoption of solid or gel substrates to anchor and assemble cells. Here, we report our experimental observations on the formation of a stable 3-D cell-assembly in bulk medium using laser tweezers without any solid/gel scaffolds, through the use of a crowding effect with macromolecules [17–19].

2. Materials and methods

NAMRU mouse mammary gland epithelial cells (NMuMG) [20] were cultured in Dulbecco's modified Eagle's medium (DMEM) (Wako Pure Chem. Ind., Japan) supplemented with 10% fetal bovine serum (FBS) (Cell Culture Biosci., Nichirei Biosci. Inc., Japan), 40 μg/ml streptomycin, and 40 units/ml penicillin (Life Tech. Corp., USA). The cells were incubated at 37 °C in a humidified atmosphere of 5% CO_2. Sub-confluent cells were harvested with trypsin (0.25% Trypsin–EDTA (1X)) (Life Tech. Corp.) and cryopreserved with CELLBANKER1 (Nippon Zenyaku Kogyo, Japan). For preparation of the crowding polymer, we used polyethylene glycol (PEG) (50,000; molecular biology-grade) (Wako Pure Chem. Ind.). We prepared 10–40 mg/ml of polymer solution with PEG (50 k) using DMEM. Microscopic images were obtained using a Nikon TE-300 inverted microscope equipped with a CCD camera (WAT-120N) (Watec Co. Ltd., Japan), and an optical laser manipulation system (Millennia IR) (Spectra-Physics. Corp., Japan) with a Nd:YAG laser

* Corresponding authors at: Laboratory of Life Physics, Faculty of Life and Medical Sciences, Doshisha University, 1-3 Tatara Miyakotani, Kyotanabe, Kyoto 6100321, Japan.

E-mail addresses: ksadakan@mail.doshisha.ac.jp (K. Sadakane), keyoshik@mail.doshisha.ac.jp (K. Yoshikawa).

http://dx.doi.org/10.1016/j.cplett.2016.05.019
0009-2614/

(cw; 1064 nm) operating between 380 and 780 mW. The optically trapped cell was transferred using an auto-stage (Sigmakoki Co. Ltd., Japan). All experiments were carried out at room temperature (23 °C).

3. Results

Fig. 1 illustrates the process by which cell–cell contact is induced through the use of laser tweezers, where (A) and (B) indi-

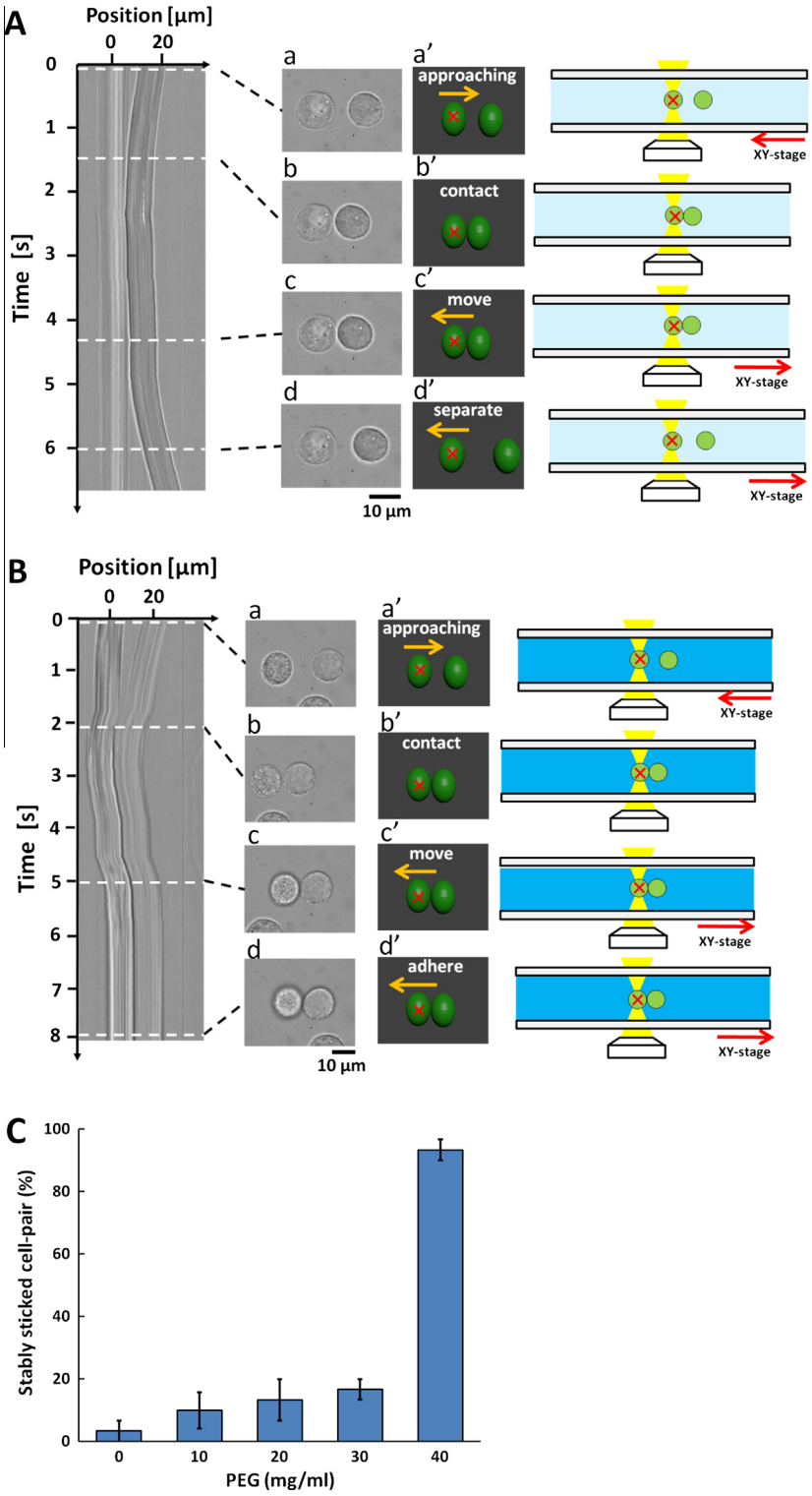

Fig. 1. Laser manipulation of a pair of epithelial cells (NMuMG); (A) in the absence and (B) in the presence of PEG (40 mg/ml): Left, spatio-temporal diagram illustrating the process of manipulation; second-left, photomicrographs of a pair of cells; third-left, schematics indicating the position of the laser focus as marked by 'x'; right, schematic illustration. (a) and (b) Transport of a targeted cell to make contact with another cell, (b) and (c) Continuation of cell–cell contact under laser tweezing, and (c) and (d) Transport of a grasped cell to the left at a speed of ca. 10 μm/s. For the schematics in a′–d′, the direction of transport of the trapped cell with respect to the cellular environment is shown, indicating the motion of cells with respect to the stage. In (A), the cell-pair separates due to viscous friction as a result of transport. In (B), the cells maintain stable contact throughout transport. (C) The probability of stable cell–cell contact being maintained through optical transport for ca. 5 μm, i.e., the percentage of experimental runs to obtain the result exemplified in (B) where the result in (A) was counted as a failure.

cate experiments with and without PEG (40 mg/ml), respectively. In these experiments, we grasp a target cell by focusing the laser and then move the cell to make contact with another desired cell. After the cells come in contact for a few seconds, the stage is moved toward the right at a speed of 10 μm/s under laser-focusing on the cell on the right. In the schematics in Fig. 1a′–d′, we indicate the trapped cell's direction of motion, relative to the cellular environment. This process exerts a viscous force on the paired cells, which can result in the pair of cells eliminating each other due to viscous friction, as shown in (A). We also confirmed that, even without external viscous friction, cell–cell contact tended to dissociate under Brownian motion once the laser was switched off. However, in the aqueous medium with PEG, cell–cell contact was maintained in a stable manner during transport in the solution, as indicated in (B). Fig. 1(C) shows the stability of cell–cell contact represented as the percentage of surviving cellular pairs after transport against viscous friction, as illustrated in Fig. 1 (A) and (B). In this measurement, cellular contact was established for 3–6 s and the cellular pair was then transferred in the solution using laser tweezers at a speed of 10 μm/s. We confirmed successful cell–cell attachment by replacing PEG with dextran (data not shown), which suggests that the present methodology is robust for achieving cell–cell contact between any two desired targets. In contrast to a previous study [8], where holographic laser tweezers were used to produce artificial cellular micro-architectures, we have here developed a novel method for generating stable cellular structures with a desired positioning between individual cells.

Next, we examined the stability of cellular attachment by transporting cell pairs from the crowding medium with polymer to a polymer-free solution. By using the experimental system shown

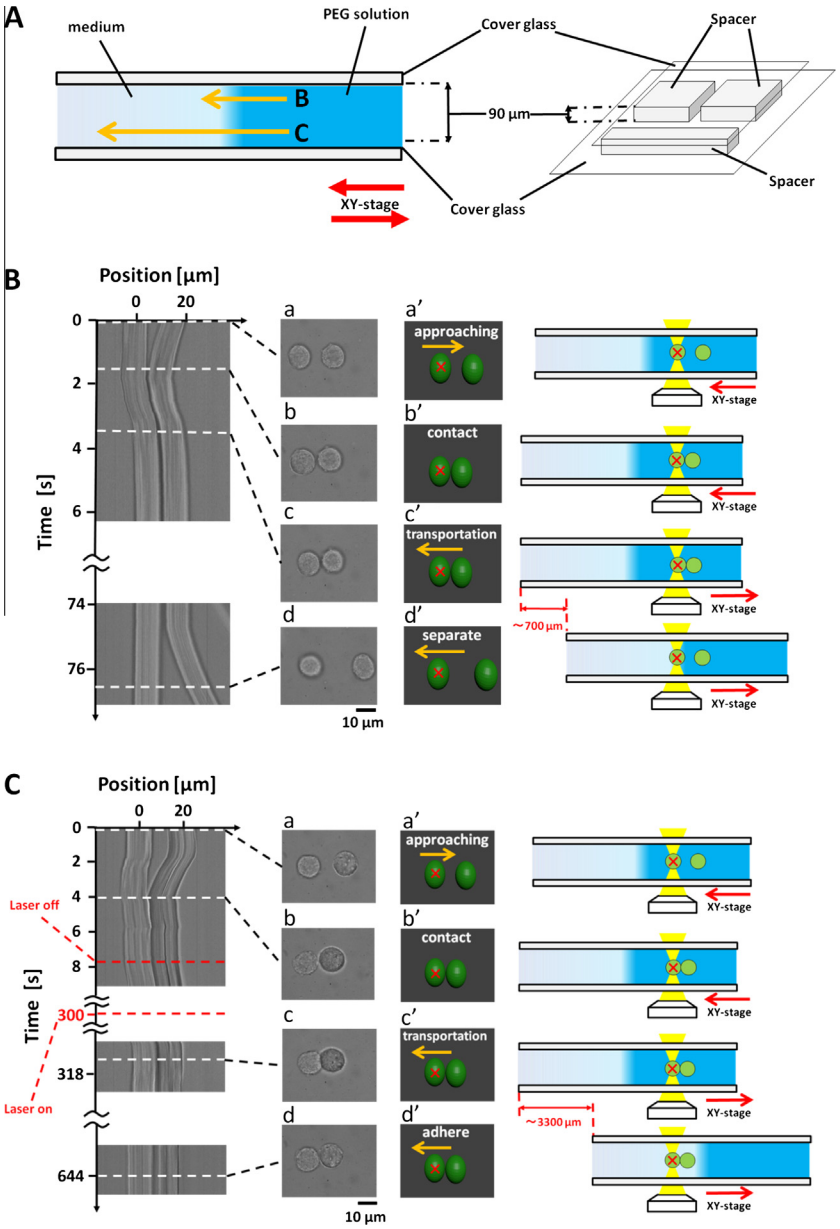

Fig. 2. Experiments to examine the stability of cell–cell contact after optical transport to a PEG-free region of the solution. (A) Experimental apparatus. (B) and (C): Dissociation and stable adhesion of cellular pairs, after ca. 2 and 290 s of contact, respectively, under laser tweezing. Left, spatiotemporal diagram; second-left, optical transport to confirm cell–cell contact in the presence of PEG solution (40 mg/ml) and transport to the PEG-free region of the medium; middle right; third-left, schematics indicating the position of the laser focus as marked by the red 'x'; left, schematic representation of the experimental procedure. Cellular pairs are transported at a speed of 10 μm/s. (For interpretation of the references to colour in this figure legend, the reader is referred to the web version of this article.)

in Fig. 2(A), we induced cell–cell contact in the region containing PEG and then transferred the cell pairs to a region without PEG, using laser tweezers. We confirmed that, under these experimental conditions, the difference in PEG concentration between the two regions was maintained for several hours. Fig. 2(B) shows the results of the transfer of the cell pairs to the region without PEG, after cellular contact was established for 3 s. Our results indicate that the cell pairs dissociated during transfer, indicating that this short contact time, on the order of seconds, was not enough to establish stable cellular attachment. On the other hand, Fig. 2(C) shows the successful transport of a cell pair to a region without PEG, where the cells were kept in contact for as long as 5 min in the region containing PEG. Taken together, these results validate that cellular contact is maintained in a stable manner.

Fig. 3 illustrates experiments that were designed to facilitate 3-D cellular assembly in a crowding environment using laser tweezers in the presence of 40 mg/ml PEG. Fig. 3(A) exemplifies the time-successive formation of a pyramidal cellular system. Fig. 3(B) shows the formation of various morphologies with multiple cells. Here, we moved the objective lens along the vertical plane to form 3-D assembly. In future experiments, it may be useful to construct twin laser foci to generate 3-D cellular assemblies.

4. Discussion

We have shown that the use of a crowding polymer solution enables the creation of a cellular assembly using laser tweezers. Here, we briefly discuss the experimental conditions needed to use the present methodology to generate a cellular assembly. It should be noted that we used a crowding polymer solution to avoid entanglement between neighboring polymer chains. Thus, the viscosity is essentially the same as that in the solution without the polymer. Under the condition that the polymer concentration exceeds that of the overlap concentration, $c*$, the transfer of individual cell pairs using the laser becomes impossible due to an increase in the solution's viscosity. Next, we discuss the occurrence of attractive interaction between cells in polymer solutions, taking into account the so-called depletion interaction [21,22].

For the stabilization energy between the facing membranes per unit area, U_a, due to the depletion effect, we may simply adopt the following theoretical model by taking the diameter 'd' of polymer coil, such as PEG, in a random coil conformation:

$$U_a = -\pi_{PEG}(2d - x) \quad \text{when} \quad x \leqslant 2d$$
$$U_a = 0 \quad \text{when} \quad x > 2d. \tag{1}$$

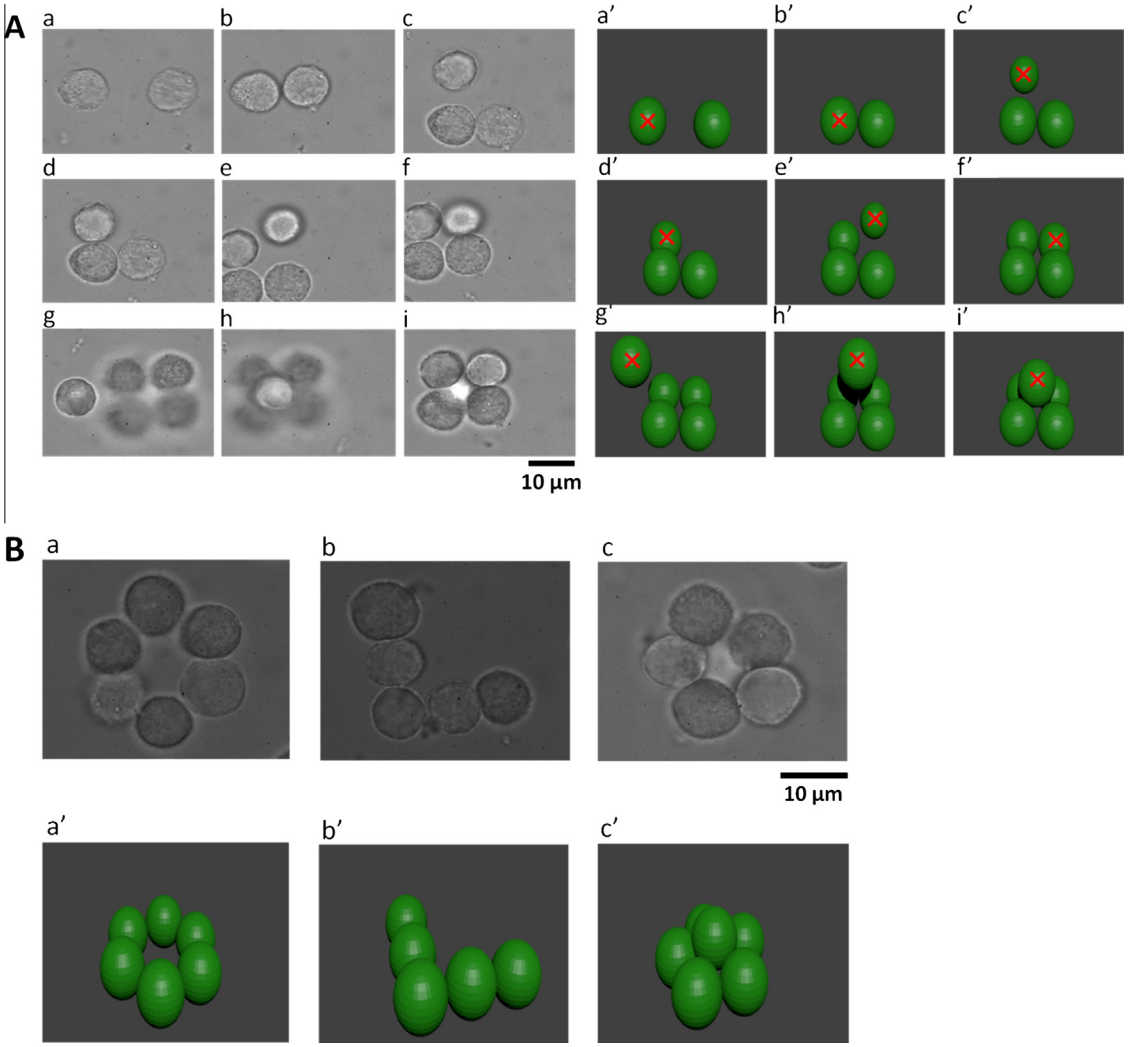

Fig. 3. Stable three-dimensional assembly of epithelial cells (NMuMG) in a medium with PEG (40 mg/ml) using laser tweezers together with schematic representations. (A) Optical construction of a pyramidal assembly. The focal point of the laser is marked by the red 'x'. (B) Examples of various cellular assemblies: a: donut, b: letter 'L', c: pentagonal pyramid as an example of 3D cluster. (For interpretation of the references to colour in this figure legend, the reader is referred to the web version of this article.)

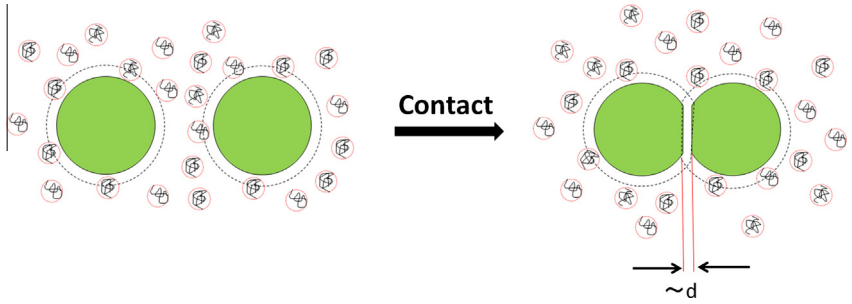

Fig. 4. Schematics representing our hypothesis for the formation of stable cell–cell contact under crowding conditions with polymers. Due to the entropic depletion force, a pair of cells forms a flat contact, with a contact area on the order of ten of μm^2. A flat gap remain between the cells with a distance corresponding to the size of the coexisting polymer molecules (~10 nm), which may contribute to the formation of stable cellular contact by keeping the cytoplasmic membrane in a fluidic state.

Several reports have discussed the subtle changes in the interaction profile due to the polymer depletion effect [23,24]. However, the essence of the interaction profile is the same, in accordance with the above simple model proposed by Asakura and Osawa [21,25]. Thus, the attractive force between the facing membranes at a distance x is expressed in terms of negative pressure:

$$P_{dep} \approx -\frac{\partial U_{\alpha}}{\partial x} = -\pi_{PEG} \quad \text{when} \quad x \leqslant 2d$$
$$P_{dep} \approx 0 \quad \text{when} \quad x > 2d, \tag{2}$$

where π_{PEG} is the osmotic pressure due to the crowding PEG. As discussed below, the osmotic pressure of crowding macromolecules becomes almost independent of the molecular weight of the crowding polymer. In other words, the pressure is simply represented by the concentration of the polymer blobs or the polymer weight concentration [24,26]. Thus, based on past reports on the measurement of the osmotic pressure of PEG [27,28], we can estimate the osmotic pressure of 40 mg/ml PEG solution to be ca. 0.02 MPa (see Fig. 1(C)).

Regarding the physicochemical mechanism that underlies the repulsive interaction between a pair of cells floating in solution, studies have been performed by taking various factors into account [29], such as electrostatic interactions between two parallel surfaces [30], electrostatic repulsion due to heterogeneous distribution of the surface charge [31], short-range hydration repulsion force [32], a glycocalyx repulsion effect [16,33], and membrane undulation [34,35]. Collectively, the results of these studies indicate the existence of short-range repulsive forces that decay more steeply with distance. For example, as a phenomenological model, Hiemenz et al. suggested [30] the following relationship for the repulsive force between the membrane surfaces of a pair of cells, represented as the positive pressure P_{rep}, with a distance x, considering electrostatic interactions together with some possible steric effect:

$$P_{rep} = P^0_{rep}\exp\left(-\frac{x}{L}\right) \tag{3}$$

where pressure P^0_{rep}, a positive variable, depends on the ionic strength of the medium and the surface potential at the extreme of $x = 0$. The characteristic length L is on the order of 1 nm for a conventional medium for cell culture, and P_{rep} is on the order of 0.1 MPa at $x = 10$ nm and 0.001 MPa at $x = 15$ nm. Although there remains some ambiguity regarding the physical origin of cell–cell repulsive interactions, such a steep decrease in the repulsive force at a length of around 10–20 nm seems to be consistent with reports in this field.

We can propose that the net pressure is the sum of the depletion and repulsive interactions:

$$P_{net} = P_{dep} + P_{rep} \tag{4}$$

As mentioned above, under our experimental conditions, $P_{dep} \sim -0.02$ MPa was sufficient to attain an effective attractive interaction between cells. Thus, it is expected that the transmembrane distance would be $x = 10$–15 nm through the balance between attractive and repulsive contributions. Here, we can evaluate the size of the polymer chain, d, in relation to the radius of gyration R_g. It would be natural to expect the following relationship: $d \approx 2R_g$. Under this assumption of a random coiled conformation, R_g can be evaluated as,

$$R_g = \sqrt{\frac{n^{2\upsilon}b^2}{6}} \tag{5}$$

where 'b' is the Kuhn length and 'n' is the number of Kuhn segments per single polymer molecule. In accordance with the interpretation in a previous study, we estimate 'b' to be 0.38 nm [36]. The parameter υ is the Flory exponent; $\upsilon = \frac{1}{2}$ for an ideal polymer and $\upsilon = \frac{3}{5}$ for a 'real' polymer. Generally, in semi-dilute regimes, the exponent tends to decrease toward 1/2 with an increase in the polymer concentration [24,26]. Here, we used PEG (50 k) (Fig. 1(C)), corresponding to a degree of polymerization of $n \sim 10^3$. Thus, we can estimate the radius of gyration to be $R_g \approx 5$ nm, under $\upsilon = \frac{1}{2}$. Accordingly, we can deduce that $d \approx 10$ nm, suggesting that, under the present experimental conditions, the distance is maintained on the order of the size of a polymer in a coil conformation.

As an additional physico-chemical parameter, it is essential to obtain larger P_{dep} values. On the other hand, viscosity should remain at the level in a usual aqueous buffer solution, to settle the desired experimental conditions for manipulation by a laser. To this end, we can use a polymer concentration that is closer to the so-called overlap concentration $c*$ (g/L = mg/mL), as in Eq. (6):

$$c^* = 3M/(4\pi N_A R_g^3) \tag{6}$$

Thus, the overlap concentration of PEG (50 k) is $c^* \sim 20$ mg/mL, where $R_g = 5$ nm (the scaling exponent, $\upsilon = \frac{1}{2}$). This suggests that $c*$ would be on the order of several tens of mg/ml under our experimental conditions.

Next, we briefly discuss the effect of cell membrane deformation, which would enable the cells to achieve flat contact with each other. The bending modulus of membranes is $\kappa \sim 10^{-19}$ J [37]. From Fig. 4, the characteristic length of the flat contact was ca. 5 μm. We estimate that the change in curvature through the formation of flat cell–cell contact was $\Delta K \approx 10^5$ m^{-1}. From this equation, we can now estimate the energy cost ε to make a flat surface:

$$\varepsilon \approx \frac{1}{2}A\kappa(\Delta K)^2 \tag{7}$$

where A is the flat contact area and is approximately ~ 20 μm^2. This indicates that the free energy penalty for deformation is on the

order of the thermal fluctuation $\varepsilon \sim k_B T$, where k_B is the Boltzmann constant and T is the absolute temperature.

Based on the above arguments, we propose a hypothesis regarding cell–cell contact interaction as represented in Fig. 4. The cytoplasmic membrane is easily deformed to allow flat cell–cell contact, which causes an inter-membrane gap on the order of R_g of the crowding polymer. We expect that such a void in the area of flat contact provides fluidity for the membrane components to decrease local repulsions and increase attractive contributions, and that, during contact for several minutes, the interacting surface of the cytoplasmic membrane acquires stability, due to the rearrangement of the facing membrane components.

5. Conclusions

In summary, we have demonstrated stable cell–cell adhesion in a crowding environment with a soluble polymer (PEG) through laser manipulation. Interestingly, after cellular contact for as long as several minutes, the contact pair retains its stability even in the absence of crowding polymers. We proposed a mechanism that could explain the stable cellular adhesion in terms of specific attractive interactions under crowding conditions, where the distance between the facing cellular membranes, with a contact area of on the length scale of several m, is maintained on the order of 10 nm, i.e., the size of a PEG molecule in a coil conformation. Our results suggest that such a specific feature of the depletion effect with a crowding polymer may allow favorable interactions between the facing membranes via the thermal fluctuation of components within cellular membranes, where 2-D fluidity is well-maintained because of the finite gap between the membranes in contact. The use of optical tweezers (Nd:YAG, wavelength 1064 nm) under a crowding environment causes no significant damage to the cells [38]. The result of the present study will stimulate the further extension of the study to examine the possible application of laser tweezers under crowding condition, such as the adhesion of cells to a tissue. Additionally, as a next step, it may be important to examine whether natural polymers can provide a suitable environment for constructing stable cellular assemblies, instead of the synthetic polymer PEG. Our preliminary experiments have shown that natural polymers, such as dextran and albumin, offer considerable promise in this direction. We hope that the application of the new methodology reported here will contribute to progress in the biological sciences, such as in the fields of tissue-engineering and regenerative medicine.

Acknowledgements

We thank Mr. Shun Watanabe for his technical assistance in this study. This work was supported by KAKENHI (15H02121, 25103012) and by the MEXT-Supported Program for the Strategic Research Foundation at Private Universities.

References

[1] Z. Ma et al., Laser patterning for the study of MSC cardiogenic differentiation at the single-cell level, Light Sci. Appl. 2 (2013) e68.
[2] H. Zhang, S. Dai, J. Bi, K.K. Liu, Biomimetic three-dimensional microenvironment for controlling stem cell fate, Interface Focus 1 (2011) 792–803.
[3] K. Muguruma, A. Nishiyama, H. Kawakami, K. Hashimoto, Y. Sasai, Self-organization of polarized cerebellar tissue in 3D culture of human pluripotent stem cells, Cell Reports 10 (2015) 537–550.
[4] T. Ohbuchi, M. Takaki, H. Misawa, H. Suzuki, Y. Ueta, In vitro morphological bud formation in organ-like three-dimensional structure from mouse ES cells induced by FGF10 signaling, Commun. Integr. Biol. 5 (2012) 312–315.
[5] K.Y. Lee, D.J. Mooney, Hydrogels for tissue engineering, Chem. Rev. 101 (2001) 1869–1879.
[6] J. Lee, M.J. Cuddihy, N.A. Kotov, Three-dimensional cell culture matrices: state of the art, Tissue Eng. B: Rev. 14 (2008) 61–86.
[7] J. Yang, M. Yamato, C. Kohno, A. Nishimoto, H. Sekine, F. Fukai, T. Okano, Cell sheet engineering: recreating tissues without biodegradable scaffolds, Biomaterials 26 (2005) 6415–6422.
[8] G.R. Kirkham, E. Britchford, T. Upton, J. Ware, G.M. Gibson, Y. Devaud, M. Ehrbar, M. Padgett, S. Allen, L.D. Buttery, K. Shakesheff, Precision assembly of complex cellular microenvironments using holographic optical tweezers, Scientific Reports 5 (2015) 8577-1–8577-7.
[9] H. Akiyama, A. Ito, Y. Kawabe, M. Kamihira, Genetically engineered angiogenic cell sheets using magnetic force-based gene delivery and tissue fabrication techniques, Biomaterials 31 (2010) 1251–1259.
[10] H. Tavana, B. Mosadegh, S. Takayama, Polymeric aqueous biphasic systems for non-contact cell printing on cells: engineering heterocellular embryonic stem cell niches, Adv. Mater. 22 (2010) 2628–2631.
[11] B. Derby, Printing and prototyping of tissues and scaffold, Science 338 (2012) 921–926.
[12] G.M. Akselrod, W. Timp, U. Mirsaidov, Q. Zhao, C. Li, R. Timp, K. Timp, P. Matsudaira, G. Timp, Laser-guided assembly of heterotypic three-dimensional living cell microarrays, Biophys. J. 91 (2006) 3465–3473.
[13] A. Ashkin, Optical trapping and manipulation of neutral particles using lasers, Proc. Natl. Acad. Sci. USA 94 (1997) 4853–4860.
[14] H. Oana, K. Kubo, K. Yoshikawa, H. Atomi, T. Imanaka, On-site manipulation of single whole-genome DNA molecules using optical tweezers, Appl. Phys. Lett. 85 (2004) 5090–5092.
[15] S. Bayoudh, T.A. Nieminen, N.R. Heckenberg, H. Rubinsztein-Dunlop, Orientation of biological cells using plane-polarized Gaussian beam optical tweezers, J. Modern Opt. 50 (2003) 1581–1590.
[16] G.I. Bell, M. Dembo, P. Bongrand, Cell adhesion: competition between nonspecific repulsion and specific bonding, Biophys. J. 45 (1984) 1051–1064.
[17] H.X. Zhou, G. Rivas, A.P. Minton, Macromolecular crowding and confinement: biochemical, biophysical, and potential physiological consequences, Annu. Rev. Biophys. 37 (2008) 375–397.
[18] K. Richter, M. Nessling, P. Lichter, Macromolecular crowding and its potential impact on nuclear function, Biochim. Biophys. Acta 1783 (2008) 2100–2107.
[19] S.B. Zimmerman, S.O. Trach, Estimation of macromolecule concentrations and excluded volume effects for the cytoplasm of *Escherichia coli*, J. Mol. Biol. 222 (1991) 599–620.
[20] G. David, B. Van der Schueren, M. Bernfield, Basal lamina formation by normal and transformed mouse mammary epithelial cells duplicated in vitro, J. Natl. Cancer Inst. 67 (1981) 719–728.
[21] S. Asakura, F. Oosawa, Surface tension of high-polymer solutions, J. Chem. Phys. 22 (1954) 1255.
[22] A.R. Khokhlov, Y.A. Grosberg, V.S. Pande, Statistical Physics of Macromolecules, American Institute of Physics, New York, 1994.
[23] R. Tuinier, J. Rieger, C.G. de Kruif, Depletion-induced phase separation in colloid-polymer mixtures, Adv. Colloid Interface Sci. 103 (2003) 1–31.
[24] I. Teraoka, Polymer Solutions: An Introduction to Physical Properties, John Wiley & Sons, Inc, New York, 2002.
[25] S. Asakura, F. Oosawa, Interaction between particles suspended in solutions of macromolecules, J. Polym. Sci. 33 (1958) 183–192.
[26] P. de Gennes, Scaling Concepts in Polymer Physics, Cornell University, New York, 1979.
[27] N.P. Money, Osmotic pressure of aqueous polyethylene glycols: relationship between molecular weight and vapor pressure deficit, Plant Physiol. 91 (1989) 766–769.
[28] C.B. Stanley, H.H. Strey, Measuring osmotic pressure of poly(ethylene glycol) solutions by sedimentation equilibrium ultracentrifugation, Macromolecules 36 (2003) 6888–6893.
[29] S. Ohki, Cell and Model Membrane Interactions, Springer, New York, 1991.
[30] P.C. Hiemenz, R. Rajagopalan, Principles of Colloid and Surface Chemistry, Marcel Dekker, Inc, New York, 1997.
[31] E. Donath, A. Voigt, Charge distribution within cell surface coats of single and interacting surfaces–a minimum free electrostatic energy approach: conclusions for electrophoretic mobility measurements, J. Theor. Biol. 101 (1983) 569–584.
[32] D.M. LeNeveu, R.P. Rand, V.A. Parsegian, Measurement of forces between lecithin bilayers, Nature 259 (1976) 601–603.
[33] G.M. Bell, S. Levine, N. McCartney, Approximate methods of determining the double-layer free energy of interaction between two charged colloidal spheres, J. Colloid Interface Sci. 33 (1970) 335–339.
[34] L. Chen, N. Jia, L. Gao, W. Fang, L. Golubovic, Effects of antimicrobial peptide revealed by simulations: translocation, pore formation, membrane corrugation and Euler buckling, Int. J. Mol. Sci. 14 (2013) 7932–7958.
[35] E. Sackmann, A.S. Smith, Physics of cell adhesion: some lessons from cell-mimetic systems, Soft Matter 10 (2014) 1644–1659.
[36] D. Marsh, Scaling and mean-field theories applied to polymer brushes, Biophys. J. 86 (2004) 2630–2633.
[37] M. Hu, P. Diggins, M. Deserno, Determining the bending modulus of a lipid membrane by simulating buckling, J. Chem. Phys. 138 (2013) 214110.
[38] H. Zhang, K.K. Liu, Optical tweezers for single cells, J. R. Soc. Interface 5 (2008) 671–690.